...ternational Journal of Modern Physics B Vol. 3, No. 1 (1989) 33–64
© World Scientific Publishing Company

PHENOMENOLOGICAL THEORY OF POLYMER MELT DYNAMICS

JEFFREY SKOLNICK*, ROBERT YARIS*
*Institute of Macromolecular Chemistry, Department of Chemistry
Washington University, St. Louis, MO 63130, USA

and

ANDRZEJ KOLINSKI
Department of Chemistry, University of Warsaw, 02-093 Warsaw, Poland

Received 16 July 1988

A particularly interesting problem in polymer physics is the mechanism by which an individual polymer chain moves in a polymer melt or concentrated polymer solution. The first rather successful model of polymer dynamics was the reptation model of de Gennes which asserts that due to the effect of entanglements a polymer finds itself confined to a tube. Thus, the dominant long wavelength motion of the chain should be slithering out the ends of the tube. In order to examine the validity of the reptation model, a series of dynamic Monte Carlo simulations were performed. Although the ...ulations are on chains sufficiently long that agreement with the experimentally observed scaling ...th degree of polymerization n of the self diffusion constant and terminal relaxation time is ...served, reptation does not appear to be the dominant mechanism of long distance motion. Rather the motion is isotropic, with the slowdown from dilute solution behavior arising from the formation of dynamic entanglements — rare long lived contacts where a given chain drags another chain through the melt for times on the order of longest internal relaxation time. Motivated by the simulations results, a phenomenological theory for the diffusive and viscoelastic behavior is developed that is consistent with both simulations and experiment and which does not invoke reptation. The major conclusions arising from the theoretical approach are described, and comparison is made with experiment.

1. Introduction

A long standing problem in polymer physics has been to develop a microscopic model for the dynamics of long chain polymer motion in melts and concentrated solutions which reproduces the experimentally seen chain length dependence of the macroscopic transport coefficients, in particular that of the diffusion constant and the shear viscosity coefficient[1–6]. Both of these quantities are observed to have universal power law dependencies on chain length — i.e. they exhibit universal scaling. The scaling behavior of the center-of-mass, self-diffusion behavior, D, in a dense solution or melt is[7–13]

$$D \sim \begin{cases} n^{-1}, & n < n_c' \\ n^{-2}, & n > n_c' \end{cases} \tag{1.1a}$$

where n is the degree of polymerization of the polymer chain, i.e., the number of monomer units per polymer chain, and n_c' is a critical degree of polymerization. The scaling behavior of the zero frequency shear viscosity, η, is[6,14]

$$\eta = \begin{cases} n^1 , n < n_c \\ n^{3.4} , n > n_c \end{cases} \tag{1.1b}$$

with the critical degrees of polymerization of the crossover for viscosity and self diffusion being unequal. Typically, $n_c' \cong 5\, n_c$.

The fact that the chain length dependence of diffusion and viscosity are universal scaling laws is a double-edged sword. Due to the universality, one explanation suffices for the whole class of polymers. Moreover, the explanation cannot depend on the details of the polymeric system, since such details change as one changes the polymer under consideration. Concomitantly, however, the information content embodied in the scaling laws is low. Hence the scaling laws themselves do not mandate the acceptance of any particular microscopic model of polymer motion. The lack of at least approximate agreement with experiment can be used to reject a particular microscopic model; however, a wide class of disparate models can (and does) lead to similar scaling laws.

Based on the changes in the scaling behavior of the melt as the polymer chain length increases, additional factors come into play; presumably these involve some aspect of interchain entanglements. The importance of these interchain entanglements in understanding polymer melt dynamics can be most graphically illustrated by the response of the melt to a sudden shear deformation[5,6]. For a short time after the deformation, the melt behaves elastically, much like a true rubber — which is a crosslinked collection of chains (i.e. the different chains in a rubber are bonded together by chemical bonds). Ultimately, however, unlike a rubber, as time goes on the polymer melt flows like a viscous liquid. Unfortunately, the exact nature of the entanglements in a melt are not agreed upon or fully understood. But based on all available experimental evidence, they appear to be extremely rare, occurring on average on the order of several hundred monomer units. Thus, the effects of interchain entanglements should be absent for short chains but become increasingly more important as the chain length increases.

The ultimate theory of polymer melt dynamics including entanglements must by the very nature of the problem be a many-body (many-chain) theory. However, for the purposes of comprehending, at least in an approximate way, what is going on in this quite complicated system, it is useful to have an effective single particle (chain) picture of the motion of a chain. This picture or model must take account of the effects of the entanglements. Before presenting an outline of our single particle picture of polymer chain dynamics, which is the main purpose of this review, it is useful to at least briefly describe two other single

particle models which have been used to describe dense polymer systems: the Rouse model[15] which is used to describe short chain, unentangled systems, and the reptation model which has been used to describe long chain, entangled systems.[1-5]

A Rouse chain is a simple bead and spring model of a polymer chain immersed in a viscous fluid[15,16]. Each monomer is represented by a bead, and each bead has associated with it a friction constant. This friction constant represents the effects of the interactions of the monomer with the surrounding fluid, be it a solvent or other polymer chains. For homopolymers (polymers composed of only a single type of monomer unit) all of the bead friction constants are the same. The connectedness of the chain is enforced by having adjacent beads in the chain joined together by Hooke's law springs. Hydrodynamic interactions, or the perturbation of the solvent velocity field at the position of one monomer due to the presence of other monomers, can be neglected for polymer melts (but not for polymers in dilute solution)[17]. Remarkably, this simple effective single particle model is a good zeroth-order representation of short (unentangled) polymer melts and yields the short chain length scaling behavior of Eqs. (1.1). In the Rouse model, the mean-square displacement of the center of mass $g_{cm} \sim 6Dt$ for all times t. In the long chain limit, the mean square displacement of a single bead (or single bead autocorrelation function) is

$$g(t) \sim t^{1/2}, \quad t < \tau_R$$
$$g(t) \sim t, \quad t > \tau_R \tag{1.2}$$

where τ_R is the terminal relaxation time of the decay of the end-to-end vector, which is the longest internal relaxation time of the polymer chain. In the Rouse model $\tau_R \sim n^2$.

In the popular and reasonably successful reptation model of polymer melt dynamics of de Gennes[1-2] and Doi and Edwards[3], it is assumed that the entanglements with other polymer chains define a tube within which a given polymer chain moves. In the original rendering of the model, the entanglements and hence the tube remains essentially static for times on the order of τ_R. Thus the many-body problem of entangled chains has been reduced to a single-chain problem — that of a chain confined to a tube. Hence, the dominant long distance motion of a chain is parallel to the original chain contour defined at zero time, i.e. it involves slithering out from the tube with lateral fluctuations being surpressed by the tube. A schematic picture of this motion is depicted in Fig. 1. The end to end vector can relax only by the chain randomly slithering out of its original (zero time) confining tube; hence the longest relaxation time of the end-to-end vector is frequently (in the context of the reptation model) called the tube renewal time.

The molecular weight dependence of the tube renewal time can easily be

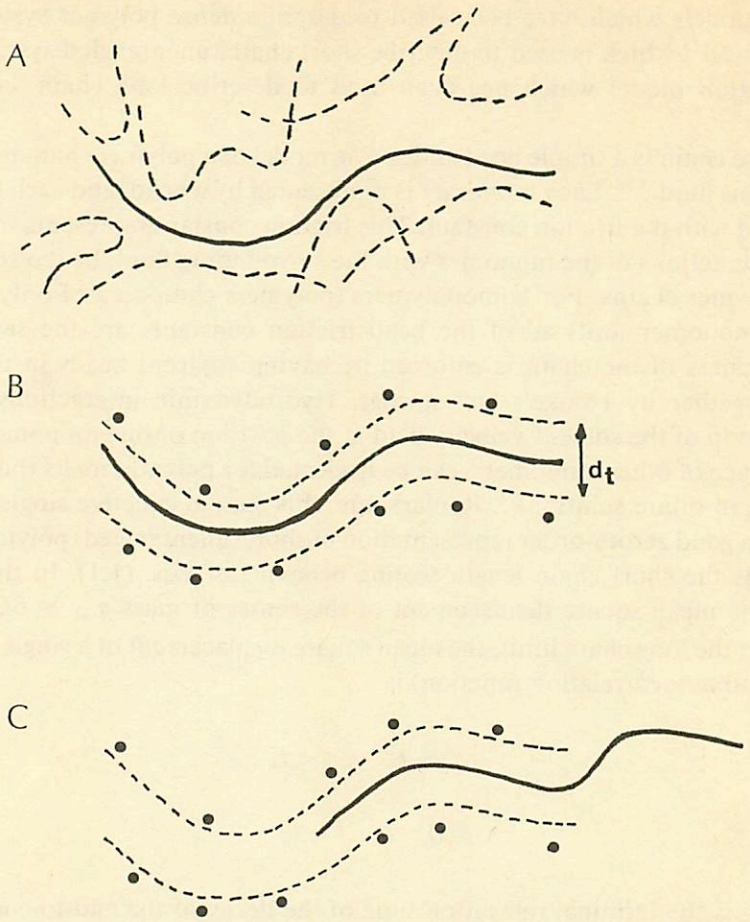

Fig. 1. Schematic representation of motion in a polymer melt as envisioned by the reptation model.

obtained by a simple scaling argument due to de Gennes[2]. If we assume that the frictional forces retarding the motion of a chain down the tube are proportional to the length of the chain, that is to n, we obtain that the mobility of the chain in the tube is inversely proportional to the friction. Hence

$$\mu \sim n^{-1} . \tag{1.3}$$

The diffusion coefficient of the chain within the tube D_{tube} (this is the diffusion constant along the curvilinear coordinate defined by the tube and is not to be confused with the measurable center of mass diffusion constant in the laboratory coordinate system to be discussed below) is related to the mobility by an Einstein relationship giving

$$D_{\text{tube}} \sim \mu \sim n^{-1} . \tag{1.4}$$

Since the time required for tube renewal is the time it takes for a chain to diffuse down the tube for a distance of the order of its chain length L, which is clearly proportional to n, in the reptation model the terminal relaxation time is given by the tube renewal time

$$\tau_R \sim L^2/D_{tube} \sim L^2 n \sim n^3 . \tag{1.5}$$

Coupled with the assumption of a rubber-like elastic response at short times[3], this leads to

$$\eta \sim \tau_R \sim n^3 . \tag{1.6}$$

This simple scaling argument for the reptation model can be continued to yield the measurable center of mass diffusion time by recognizing that in a time τ_R the chain has diffused a distance L ($\sim n$) along the curvilinear path defined by the tube. However, this path is a highly contorted tortuous path when viewed in the laboratory coordinate system. Assuming ideal (Gaussian) chain statistics, the average distance diffused in the laboratory coordinate system in a time τ_R is

$$R_0 \sim L^{1/2} \sim n^{1/2} . \tag{1.7}$$

This leads to a translational diffusion coefficient (in the laboratory coordinate system)

$$D \sim \frac{R_0^2}{\tau_R} \sim \frac{n}{\tau_R} \sim n^{-2} . \tag{1.8}$$

Thus this simple, single particle, reptation model yields results for the transport properties Eqs. (1.6) and (1.8), which are close to reproducing the experimental results of Eqs. (1.1).

For the reptation model, the behavior of the single bead autocorrelation function is more complicated than for the Rouse model of a free chain (Eq. (1.2)). For times short enough such that the mean square displacement of a bead, $g(t)$, is less than the tube diameter, the system does not know there is a tube and behaves like a free Rouse chain,

$$g(t) \sim t^{1/2} , \; g(t) < \text{mean square tube diameter} . \tag{1.9a}$$

In the next regime the chain now feels the tube and equilibrates within the tube by "defect diffusion" along the tube. This process is essentially the motion of a free Rouse one-dimensional chain confined to a Gaussian tube. Hence

$$g(t) \sim t^{1/4} , \; t < \text{defect diffusion time} . \tag{1.9b}$$

This $t^{1/4}$ regime for $g(t)$ has frequently been treated as a "signature" of reptation and will be discussed further in Sect. 2. In the next time regime, after the chain has equilibrated in the tube, its motion is characterized by the center of mass diffusion of the whole chain along the path of the Gaussian tube until the tube renewal time, hence

$$g(t) \sim t^{1/2}, t \begin{cases} > \text{defect diffusion time} \\ < \text{tube renewal time} \end{cases} . \tag{1.9c}$$

Finally, when t is greater than the tube renewal time $g(t)$ exhibits free diffusion behavior, i.e.

$$g(t) \sim t, \quad t > \text{tube renewal time.} \tag{1.9d}$$

More recent developments in the reptation model relax the requirement that the entanglements behave statically and allow the confining chains to also reptate — thus all chains are treated in a self consistent manner[18–19]. Allowances were also made for a small amount of "tube leakage"[5,20]. However, the confining tube which supresses lateral fluctuations remains the feature which all reptation treatments have in common. Thus, they all predict that if we could follow the time trajectory of a chain in a melt, its long time motion (i.e. $t >$ defect diffusion time but less than tube renewal time) would be predominantly parallel to its zero time contour.

The molecular weight dependence of the macroscopic transport coefficients can be employed to examine whether a particular realization of the dynamics is in accord with experiment, but reproducing the correct scaling behavior by no means guarantees that the particular assumptions of the model are correct. Many different models in fact give rise to similar scaling behavior. Therefore, in order to better understand the nature of the chain dynamics from a more fundamental level, we undertook a series of large scale dynamic Monte Carlo simulations of dense systems of long polymer chains[21]. We view these simulations as an experiment, albeit a computational rather than a physical experiment. A major benefit of doing computational experiments is that one can ask the simulation questions that real experimentalists do not at present know how to answer (or even ask). In particular, we can look at the time trajectory of a chain's motion in order to see if in fact it is reptating. If we find that it is not reptating — as we did — we can then look to see what the motion is and how we can describe it. We can also look at the simulation to find features that allow for simplification of the theoretical description of the dynamics of polymer melt motion. Since our model of polymer melt dynamics, which forms the main topic of this review, is founded on these simulations in that the key assumptions of the model are justified by the simulations, we include a brief summary of the main simulation results in Sect. 2

of this review. For further details, we refer the reader to the original papers[21] and to a short review that has recently appeared[22]

The major focus of this review is the presentation of a phenomenological model of melt dynamics that is in accord with all the major experimental and simulation results[23]. The fundamental premise is that entanglements are intrinsically dynamical in nature and arise from rare long lived contacts between pairs of chains. In essence, a given chain drags another chain with it for times on the order of the longest internal relaxation time of the system; subsequently, the entanglement dissolves and others form. The outline of the remainder of this paper is as follows: The development of the phenomenological theory is split into two parts: a treatment of diffusion (Sect. 3), and a treatment of viscoelasticity (Sect. 4). This review will only discuss the physical description of the model and present the major results of the theory. For readers who desire to see the detailed mathematical development, we refer to the original papers.[21-24]

2. Results of Computer Simulations

Lattice dynamic Monte Carlo simulations were performed for homopolymeric chains on a diamond lattice of degree of polymerization up to 216 over a range of volume fraction of occupied sites, ϕ, ranging from 0.0 (isolated chains) to 0.75[21b] and for homopolymeric chains on a cubic lattice at a fixed $\phi = 0.5$ for chains from $n = 64$ to 800[21c]. We also studied the properties of a test chain having $n_p = 100$ in a matrix of chains whose degree of polymerization ranged from $n_m = 50$ to 800 on a cubic lattice at $\phi = 0.5$[21d]. In all cases, excluded volume effects were included by prohibiting the multiple occupancy of lattice sites. For a detailed description of the local Monte Carlo moves see Ref. 21b for the diamond lattice and Ref. 21c for the cubic lattice. The diamond and cubic lattice simulations yield identical results for dynamic quantities when corrected for the difference in the local persistence length (a chain of size n on a cubic lattice behaves dynamically roughly like a chain of size $n/2$ on a diamond lattice).

Major Results

1. By suitably averaging the local dynamics of the chain to eliminate the effect of irrelevant local fluctuations in conformation, we were able to determine a "primitive path", in the sense of Edwards[3,25], for each individual chain in the dense system of chains and also the time trajectory of each primitive path. Thus we could study the time development of the primitive path to see how the chains were moving in the melt. An example of the time evolution of a primitive path is given in Fig. 2 where the zero time path is the thin line and the path at a later time (less than the terminal relaxation time or tube renewal time of reptation theory) is the thick line. Hence by reptation theory, at least, the central protion of the chain would have to be slithering in the tube. Figure 2 shows no evidence that this is the case (for other examples of the time development of the primitive path see Refs.

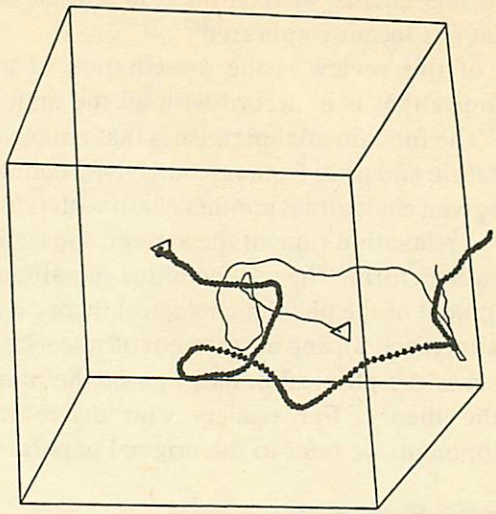

Fig. 2. Representative snapshop projections of the equivalent path for a chain of $n = 800$ on a cubic lattice polymer melt at $\phi = 0.5$. The thin curve is the primitive path defined at zero time and the thick curve defined by the overlapping circles (blobs) is the primitive path 1.2×10^5 steps later. The triangle labels one chain end.

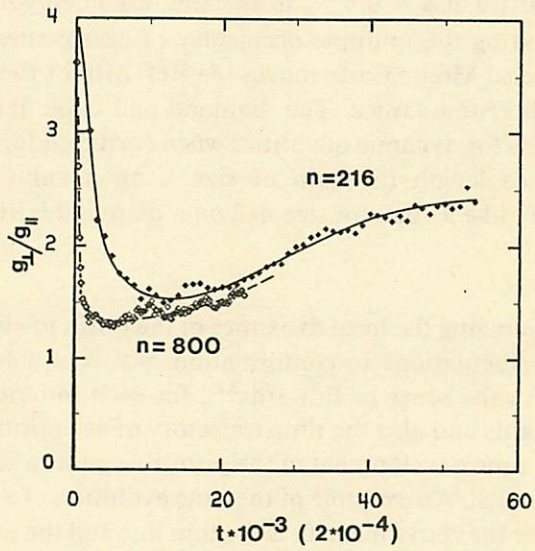

Fig. 3. Plot of the ratio $g_\perp(t)/g_\parallel(t)$ vs. time $\times 10^{-3}$ (2×10^{-4}) for $n = 216$ (800) in the upper (lower) curve. Both are at a density of $\phi = 0.5$ on a cubic lattice.

21b-d). Looking at pictures of the primitive path evolution can give one a qualitative feel for the motion of a chain. However, in order to be really sure that the chains were not reptating we sought a quantitative measure of their motion. We remind the readers that the primitive path defines the curvilinear coordinate system down which the chain would reptate if reptation were the dominant motion. Thus, by taking the path of a given chain at some time, $t = 0$, as a curvilinear coordinate, we could project the path at a latter time back on to the $t = 0$ primitive path and then determine whether the diffusive motion was predominantly parallel to the initial path (as would be required by the reptation model). Let $g_{\parallel}(t)$ be the mean square displacement down the original contour defined at zero time (the reptation component) and $g_{\perp}(t)$ be the mean square displacement perpendicular to the contour defined at zero time. Figure 3 is a plot of $g_{\perp}/g_{\parallel}$ vs. time for chains of $n = 216$ (solid diamonds) and 800 (open diamonds) beads, each in a homopolymeric cubic lattice melt at $\phi = 0.50$. If the reptation model were correct, transverse motion would be suppressed, and $g_{\perp}/g_{\parallel}$ would be a monotonically decreasing function of time. Instead, we see that after a short time (the short time results are a local cooperative dynamics effect)[21a], $g_{\perp}/g_{\parallel}$ is a monotonically increasing function of time. This result is consistent with isotropic chain motion. Identical results were found for the diamond lattice at other chain lengths[21b], and for short probe chains in a melt of longer chains.[21d]

As a check that our Monte Carlo moves were not somehow suppressing longitudinal motion, we did the experiment of simulating a single mobile chain[21b] in an environment of partially frozen chains, a situation where chains are known to reptate.[26–29] This was done on a diamond lattice for a single mobile chain of $n = 216$ imbedded in a matrix of chains which are pinned every 18 beads, with all of the other beads free to move with the same dynamics as in the melt simulation algorithm. The overall chain density ϕ is 0.5. In Fig. 4 we show $g_{\perp}/g_{\parallel}$ as a function of time for a mobile chain in a partially frozen environment and indeed it is a monotonically decreasing function of time, characteristic of reptating chains in contrast to the case of completely mobile chains shown in Fig. 3 (similar results were observed for a mobile chain of $n = 100$). It should be mentioned that although in a partially frozen environment reptation definitely was the dominant mode of diffusive motion an examination of the trajectories shows that considerable tube leakage occurs.

Hence, we were forced to conclude that, at least for the range of chain lengths we could simulate, reptation was not the dominant mode of diffusive motion, and we should look for another explanation for the transport properties of polymer melts.

2. The molecular weight dependence of the simulated homopolymeric melt self diffusion constant is fit quite well by a function

$$D = d_0/n\,(1 + n/n_e)\,. \tag{2.1}$$

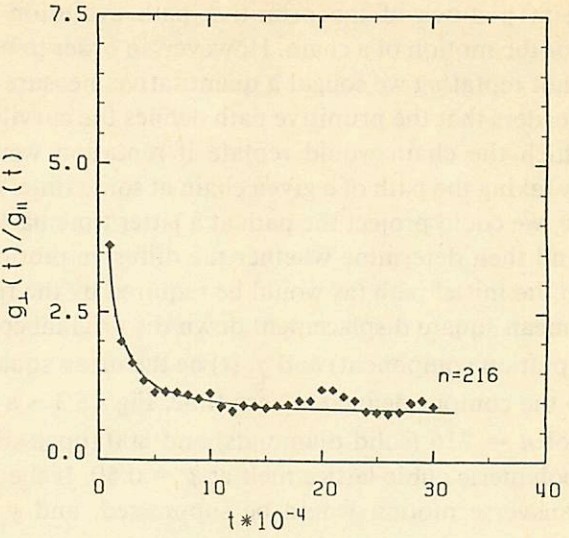

Fig. 4. Plot of the ratio of $g_\perp(t)/g_\parallel(t)$ vs. time $\times 10^{-4}$ for a single chain of $n = 216$ in a partially frozen matrix of other chains pinned every 18 beads and at an overall density of $\phi = 0.5$ on a diamond lattice.

Anticipating a result from the theory, d_0 should be interpreted as a monomeric self-diffusion coefficient (i.e., the diffusion coefficient a monomer would have in the absence of chain connectivity), and n_e will be interpreted as an entanglement length (the average number of monomers between entanglements). Hence, the simulations clearly give the correct short chain experimental results $D \sim n^{-1}$ when $n \ll n_e$ and the correct long chain experimental results ($D \sim n^{-2}$) when $n \gg n_e$ (see Eq. (1.1a)). Fitting Eq. (2.1) to the cubic lattice simulations gives $n_e = 125$, a number of the correct order of magnitude.

3. In order to obtain a better understanding of the nature of the entanglements (static vs. dynamic) we looked at the time development of interchain contacts[23]. Unfortunately, at present this is a quantity that is completely inaccessible from experiment. Each chain is replaced by a non-overlapping pearl necklace model where each pearl contains the number of monomer untis over which static excluded volume effects are felt (i.e. the static excluded volume screening length). We then searched for pairs of pearls, each on a different chain, such that the pearls are in contact at time zero (more precisely, their centers are within a specified distance of each other). By counting the fraction of such contacts that still survive up to a later time t in an $n = 216$, $\phi = 0.5$ cubic lattice melt, we determined that 64% of the contacts decay within 1% of τ_R, 91% of the contacts have decayed within 9% of τ_R, but the remaining 9% of the contacts live a time of the order of τ_R. Since τ_R is the longest relaxation time for a polymer chain and is of the order of the time scale for hydrodynamic properties such as diffusion and vis-

cosity, it is only the long lived contacts, which we call dynamic entanglements, which explicitly affect the hydrodynamic properties. The short lived contacts can be disposed of by a standard separation of time scales argument and their effect included in a monomeric friction term. If one evaluates the mean distance between dynamic entanglements for a cubic lattice chain, it is 133 monomer units. Note that this is essentially the same result obtained for n_e (125) by fitting Eq. (2.1) to the computed chain length dependence of the diffusion constant.

4. The product $D\ \tau_R/\langle S^2\rangle \sim n^\alpha$, where $\langle S^2\rangle$ is the mean square radius of gyration of the chain, and $\alpha = 0.2 \pm .05$ for a diamond lattice[21b] and $0.1 \pm .05$ for a cubic lattice[21c]. This result is similar to that seen experimentally $\eta D/\langle S^2\rangle \sim n^{0.4}$ if τ_R is assumed to be proportional to η.[5,6]

5. The results of the simulations are not in agreement with either of the standard simple single particle models of chain behavior, the reptation model which has been used in the entangled regime, or the Rouse model which has been used in the unentangled regime. However, for entangled systems, the simulation results are closer to a Rouse chain than to a reptation model. Given the appeal of an effective single particle picture, a generalization of the Rouse model appears to be reasonable.

A question that must always be addressed in using the results of a simulation to obtain insight about the dynamics of a polymer melt is whether the chains are long enough and the density high enough to reasonably represent the relevant physics. This question can be addressed in several ways. The first, and probably most naive, answer is that the simulations reproduce the experimentally observed results for the transport properties. The second way to address this question is by describing static screening lengths and persistence lengths. However, this somewhat begs the main question about dynamics. The most relevant question is to ask how entangled are the simulated chains. In asking this question the density and the chain length must be considered together, since obviously for a given chain length by increasing the density one can increase the average number of entanglements per chain (and similarly at a given density the number of entanglements per chain depends on the chain length).

For our simulations on a cubic lattice at a density of $\phi = 0.5$, we obtained a mean distance between entanglements of 130 monomers units in three independent ways. The first two were obtained by looking at the number of long lived contacts and fitting the homopolymeric melt self-diffusion constant, as described above. The third determination[21d] was by fitting the diffusion constant of a probe chain of $n_p = 100$ in a matrix of chains whose degree of polymerization ranged from $n_m = 50$ to 800, all at $\phi = 0.5$, to the theory discussed below in Sect. 3. Since the average distance between entanglements is 130 monomer units, this means that our longest simulated chains, $n = 800$ on a cubic lattice at a density of $\phi = 0.5$ have an average of slightly over 6 entanglements per chain.

To get some physical feeling for this in terms of a real polymer, the

experimentally obtained entanglement molecular weight for a polystyrene melt is 18,000 (a brief discussion of how this is obtained is given in Sect. 3). If we simply scale the mean number of entanglements per chain to the experimental entanglement molecular weight, our longest simulations of $n = 800$ at $\phi = 0.5$ corresponds to a polystyrene melt with a molecular weight of just over 110,000. While we are by no means claiming that our simulations have reached asymptotia (a claim we have no idea how we could ever independently substantiate) they clearly correspond to a quite respectable, entangled polymer melt well within the range studied by experimentalists.

In this context, we should mention the very recent, massive, molecular dynamics simulations of polymer melts by Kremer and coworkers[30]. They opted for shorter chains, their longest being 150 monomers units, and a higher density, 0.85, in the standard reduced Lennard-Jones units (where the Lennard-Jones potential distance parameters $\sigma = 1$), than we did. They provide two different estimates of the entanglement length n_e. The first $n_e \simeq 110$, obtained by fitting their diffusion data, they reject as being too high. The second, obtained by fitting the simulated single bead autocorrelation function to the reptation model, gave $n_e \simeq 35$, a result the authors preferred. From their preferred value of the entanglement length they obtain an average number of entanglements per chain of slightly more than 4 for their longest simulated chains. This scales to a molecular weight of just over 77,000 for polystyrene.

Kremer and coworkers[30] interpret the fact that they obtain a $t^{1/4}$ regime of the single bead autocorrelation averaged over the five central beads of their longest chain ($n = 150$) as evidence for the reptation model (see Eq. (1.9b)). They also point out that when the autocorrelation function is averaged over the whole chain a clean $t^{1/4}$ regime is not observed due to the added mobility of the ends. In our simulations we calculated the single bead autocorrelation function averaging over all of the beads (thus including the more mobile end motion). For a chain of 800 beads we obtained a plateau value of $t^{0.360 \pm 0.008}$ (see Fig. 4 and Table 3 of Ref. 21c). If we only average over the central five beads we obtain a $t^{0.28}$ regime for the autocorrelation function for both the $n = 216$ and the $n = 800$ chains. However these chains were not shown to be reptating by the primitive path analysis described above (see Fig. 3). Similarly, taking our analytic model of a chain with a set of high frictional (slow moving) points described in Sect. 4 (which also qualitatively agrees with the experimental results) we obtained a $t^{0.28}$ regime for the single bead autocorrelation function (averaged over all of the beads) for a chain with 17 entanglements (see Table 3 of Ref. 24). Here again the analytic model, by construction, does not reptate. Hence, we do not regard the presence of a $t^{1/4}$ regime in the single bead autocorrelation function as evidence for the reptation model since it clearly can be, and has been, obtained in the absence of reptation. In this regard it is similar to the n^{-2} scaling of diffusion, it is permissive, but by no means compulsive, evidence for the physical correctness of the reptation picture.

Hence, in the absence of a primitive path analysis as described above, or some other analysis of the computed trajectory, it still remains to be seen whether the simulations of Kremer and coworkers[30] do, or do not, support the reptation model.

3. Diffusion

Our treatment of self diffusion in polymer melts is patterned after Hess' generalized Rouse treatment which he used to justify reptation-like behavior[31]. Having the insight afforded by our simulations, we were able to make a physically more realistic set of assumptions which leads to an analytic theory in agreement with both experiments and the simulations. In particular, Hess assumed[31] that the forces are perpendicular to the chain axis, thus arriving at a reptation-like diffusion. He further factored the motion (or more specifically the propagator of the motion) into the product of a parallel (to the chain axis) and a perpendicular component and weakly coupled the perpendicular and parallel modes. We, on the other hand[23], following closely our simulation results, which indicated that over the relevant time scale the behavior of the chains is essentially Rouse-like, factor the motion (the propagator) into a product of the center of mass motion and the motion of the internal (Rouse-like) coordinates and allow for a weak coupling between them.

Starting from the Green-Kubo expression for the diffusion constant

$$D = \frac{1}{3}\int_0^\infty dt \langle \mathbf{v}(t) \cdot \mathbf{v}(o)\rangle \tag{3.1}$$

where $\langle \mathbf{v}(t) \cdot \mathbf{v}(o)\rangle$ is the velocity autocorrelation function, and using a Zwanzig-Mori projection operator treatment yields

$$D = k_B T/n\left[\zeta_o + \int_0^\infty dt \Delta\zeta(t)\right]. \tag{3.2}$$

Here ζ_0 is a generalized, concentration dependent Rouse-Zimm monomer friction coefficient and $\Delta\zeta$ is a dynamic friction term due to the interaction between different polymer chains. By invoking the standard separation of time scales argument, the effects of the short-lived interchain contacts can be averaged over, thereby yielding a renormalized Rouse-Zimm monomer friction constant, ζ_0. This leaves only the long lived, dilute, dynamic entanglements to be treated in $\Delta\zeta$, which is given by

$$\Delta\zeta(t) = \langle(\mathbf{F}(t) \cdot \mathbf{F}(o)\rangle/3nk_B T, \tag{3.3}$$

where the correlation function is a Zwanzig-Mori projected force autocorrelation function.

One now makes the following simplifying physical assumptions:
i) The interactions between polymer chains are short ranged, steric (excluded volume, replusive) interactions. This assumes that long ranged hydrodynamic interactions are completely screened[17] and that to a first approximation one can neglect attractive interactions, except insofar as they are included in the renormalized monomer friction constant.
ii) The dynamic evolution of the friction constant $\Delta\zeta(t)$ is identified with the dynamic evolution of the dynamic entanglements between chains.
iii) Since dynamic entanglements are dilute, the global motion of the chains can be treated as uncorrelated, and the interaction hierarchy can be safely truncated at the pair level, i.e. correlated three-body interactions are neglected.

The time evolution of dynamic entanglements is treated in terms of a propagator, $R(q,t)$, for the pair of chains in contact. Since one is only interested in the diffusional behavior of the polymers, the propagator need only be considered in the long wavelength, hydrodynamic limit, where the hydrodynamic pole dominates. Thus,

$$R(q,t) = \exp(-D_{\text{eff}}\, q^2 t)\,. \tag{3.4}$$

Here D_{eff} is an effective diffusion constant and q is the magnitude of the wave vector.

From our simulation results, we know that we need the propagator evaluated for times on the order of the terminal relaxation time. For times greater than τ_R, the dynamic entanglements have come apart and for times considerably less than τ_R, the effects of contacts are included in ζ_0. In this time regime, the simulations show that the behavior of the chains is essentially Rouse-like (see for example Fig. 15 of Ref. 21b and the discussion therein) with a small coupling between the center-of-mass coordinate and the internal, Rouse-like, coordinates. This physics can be introduced into the model by making further the assumption that

iv)
$$D_{\text{eff}} = (1-\beta)D_0 + \beta D \tag{3.5}$$

where D_0 is the renormalized Rouse diffusion constant given by

$$D_0 = \frac{k_B T}{n\zeta_0} = \frac{d_0}{n}\,, \tag{3.6}$$

D is the center-of-mass diffusion constant and β, which is small in the melt regime, gives the coupling between the center-of-mass motion and the internal dynamics.

From these physical assumptions and the general Hess treatment, we arrive at an implicit equation for the self-diffusion constant

$$D = D_0\{1 + \psi(c, n)[(1 - \beta)D_0 + \beta D]^{-1}\}^{-1}. \tag{3.7}$$

$\psi(c, n)$ is related to the free energy change per chain per dynamic entanglement and must be proportional to the number of dynamic entanglements per chain. Thus we define the dynamic entanglement length by

$$\psi = n/n_e. \tag{3.8}$$

n_e can be shown to be inversely proportional to c, the concentration of polymer segments per unit volume.[23]

Inserting Eqs. (3.6) and (3.8) into Eq. (3.7) and explicitly solving for D gives

$$D = D_0\left(2(1-\beta)\{(1-2\beta + n/n_e) + [1+2(1-2\beta)(n/n_e) + (n/n_e)^2]^{1/2}\}^{-1}\right). \tag{3.9}$$

If we neglect the small coupling (small β) between the internal and external coordinates in Eq. (3.9) we obtain

$$D = \frac{d_0}{n(1+n/n_e)},$$

giving Eq. (2.1) which was used to empirically fit the simulation data giving $d_0 = 0.16$ and $n_e = 125$. For all β, if the chain length is small, i.e. $n/n_e \to 0$, we obtain the free Rouse behavior

$$D = D_0 = \frac{d_0}{n}, \qquad (n < n_e) \tag{3.10a}$$

and for all $\beta \neq 1$ when the chain length is large, i.e. $n/n_e \to \infty$, we obtain

$$D = d_0(1-\beta)n_e/n^2, \qquad (n < n_e). \tag{3.10b}$$

Equations (3.10a) and (3.10b) recover the experimental results of Eq. (1.1a).

Furthermore, in the limit that $\beta \to 1$, Eq. (3.9) gives

$$D = \begin{cases} d_0/n(1 - n/n_e), & n \leq n_e \\ 0, & n \geq n_e \end{cases}. \tag{3.11}$$

Since the shutting down of long wavelength, diffusional modes signals the onset of the glass transition, Eq. (3.11) predicts a glass transition when $\beta = 1$ and $n \geq n_e$. The glass transition occurs because, when $\beta = 1$, the propagator for dynamic contacts given by Eq. (3.4) has $D_{\text{eff}} = D$. Thus, in this limit the system is so

tightly coupled that even the short time propagator requires the full center-of-mass diffusion constant instead of the "free" Rouse propagator. Each chain pulls another chain, which pulls another chain, etc. The shutting down of the diffusional modes signaled by $D = 0$ shows that the tightly coupled system is no longer a melt but a glass. Qualitatively then, high molecular weight, entangled polymeric systems undergo a glass transition when the dynamic entanglements become trapped, i.e. the global mode which allows for dynamic entanglement disengagements shuts down. This requires us to consider the coupling constant β to be a function of concentration and temperature. Polymers which are below the entanglement molecular weight do not have the entanglement trapping mechanism available to them as a means of shutting down the hydrodynamic, diffusional modes. They go through a glass transition when local, conformational changing volume fluctuations shut down; a particular example of this was seen in our diamond lattice Monte Carlo simulations[21a]. This is consistent with the experimental observation that high molecular weight polymer melts have a molecular weight independent glass transition temperature, while for low molecular weight melts (i.e. chains shorter than the entanglement length) the glass transition temperature is considerably lower.[32]

The above treatment of polymer melt diffusion can easily be extended to the case where a probe polymer of degree of polymerization n_p diffuses in a melt of polymers of degree of polymerization n_m. The analysis of this situation only differs from the above in that the dynamic friction of the probe chain arises from dyamic entanglements between the probe polymer and matrix polymers (assuming that the concentration of probe chains is small enough that probe-probe interactions can be neglected — further generalization is straightforward). This requires that in Eq. (3.4) for the propagator, we use the effective diffusion constant for a probe-matrix pair. Employing the same physics which led to Eq. (3.5) in the monodispersed melt we obtain

$$D_{\text{eff}} = (1 - \beta)[\gamma D_{0p} + (1 - \gamma)D_{0m}] + \beta(\gamma' D_p + (1 - \gamma')D_m), \tag{3.12a}$$

where p(m) denotes a probe (matrix) polymer chain, D_0 again is the renormalized Rouse diffusion constant and D is the center-of-mass diffusion constant. In the long time asymptotic regime, a mutual diffusion constant is just the average of the diffusion constants, but since we do not really know how to take averages in the intermediate time regime described by the propagator we leave γ and γ' as adjustable constants to be fit by experiment. However, we do not expect that γ and γ' should differ significantly from their asymptotic value of 1/2. When we fit our simulations using γ as a free parameter, we only obtained a slightly better fit than using the asymptotic value of 1/2. Moreover, β, the coupling between the center-of-mass and internal modes is small, and we could fit the simulation results for

monodisperse systems using $\beta = 0$. Emboldened by these results, we shall use the approximation that the asymptotic averaging applies (i.e. $\gamma = \gamma' \simeq 1/2$) and that as long as we stay away from the glass transition we can neglect the small coupling between internal and external modes (i.e. $\beta = 0$). Hence

$$D_{\text{eff}} = 1/2[D_{0\text{p}} + D_{0\text{m}}]\,. \tag{3.12b}$$

Using this result in the general Hess treatment yields

$$D_{\text{p}} = \frac{d_0}{n_{\text{p}}}\left[\frac{1 + n_{\text{p}}/n_{\text{m}}}{1 + n_{\text{p}}/n_{\text{m}} + 2\,n_{\text{p}}/n_{\text{e}}}\right]. \tag{3.13}$$

A complete treatment using the full Eq. (3.12a) for the propagator is given in Ref. 23. In the monodisperse limit where $n_{\text{p}}/n_{\text{m}} \to 1$, Eq. (3.13) goes over to Eq. (2.1).

The most stringent comparison of Eq. (3.13) and the simulation was to take d_0 and n_{e} from the simulations on monodispersed melts and calculate the diffusion of a probe chain using no adjustable parameters. The resulting average error in the fit was only about 1.5 times the statistical error in the simulation.

Comparison with experiment

In order to see whether our diffusion theory fit real experimental data as well as it did our computational experiments, we used the recent experiments of Antonietti, Folsch and Sillescu on polystyrene melts[13]. They measured the self-diffusion constants for 10 different molecular weight melts ranging from 7,200 to 75,400 at two different temperatures 180°C and 212°C (both well above the glass transition temperature of polystyrene of 100°C)[33]. They also used the same molecular weight samples dissolved in a polystyrene matrix of molecular weight 111,000 to measure the probe diffusion constants at the same two temperatures.

The experimental entanglement molecular weight for polystyrene is 18,000 which is obtained using[6,12]

$$M_{\text{e}} = c\frac{RT}{G_N^0} \tag{3.14}$$

where c is the mass/unit volume of chains, R is the gas constant, T is the temperature and G_N^0 is the plateau modulus of the species (which is molecular weight independent). Dividing the experimental entanglement molecular weight by the molecular weight of monomeric styrene produces an experimental value of n_{e} equal to 173. Hence the polystyrene samples Sillescu and coworkers use for their melt diffusion measurements range from $n/n_{\text{e}} = 0.4$ to $n/n_{\text{e}} = 4.2$. These measurements should be a good test of the theory since they are in the crossover

regime between unentangled and entangled chains. (We already know the theory fits both extremes.)

To make the comparison with experiment as tough as possible on the theory, we used the smallest possible number of free parameters[34]. That is, we used Eq. (2.1) for the self diffusion constant of a neat polymer melt and Eq. (3.13) for the diffusion of a probe chain. Hence, we neglected the coupling of internal and external modes by setting $\beta = 0$ and used the asymptotic value of $\gamma = 1/2$. We used the experimental value of $n_e = 173$ throughout, thus leaving d_0, the monomeric diffusion constant, as the only free parameter. From the meaning of d_0, it should be molecular weight independent and independent of the molecular weight of the matrix in which a probe chain is dissolved. However d_0 is temperature dependent. Hence, we used the same d_0 to fit both the self diffusion and probe diffusion data but used a different d_0 at each of the two temperatures.

The resulting comparison between theory and experiment are given in Fig. 5 for the self diffusion and Fig. 6 for the probe diffusion. The theory is in quite good

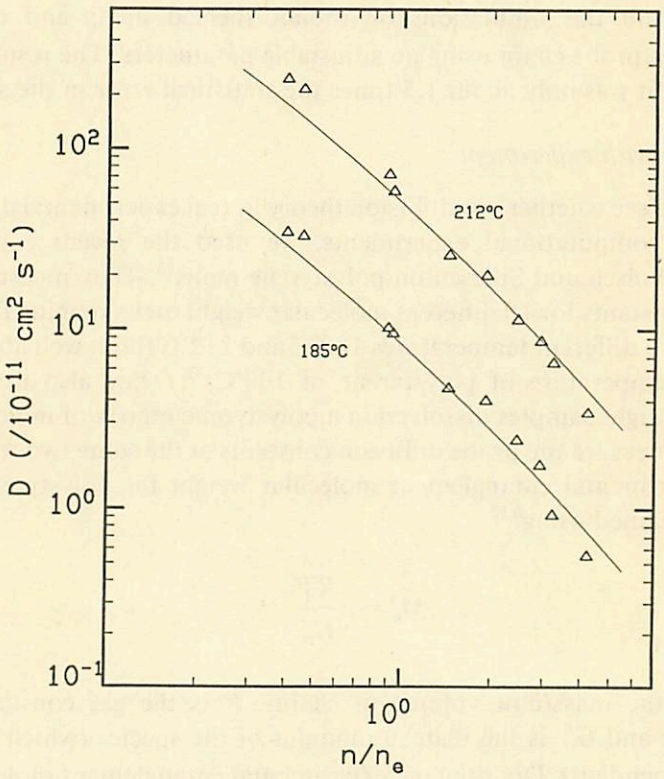

Fig. 5. Log-log plot of the homopolyer self-diffusion constant vs. n/n_e at 180°C and 212°C, in the upper and lower set of curves. The open triangles are the data of Antonietti, Folsch and Sillescu[13]; the solid curve is the fit of Eq. (2.1) to experiment.

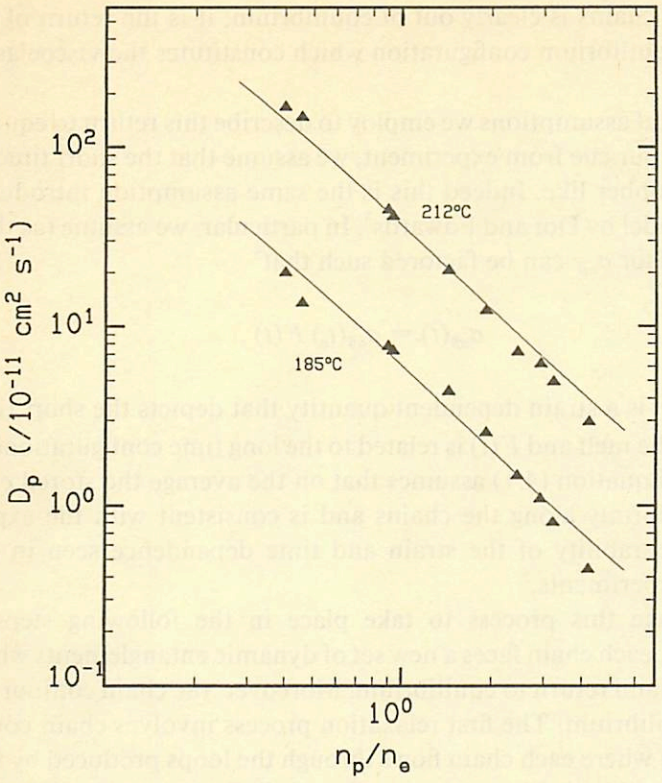

Fig. 6. Log-log plot of probe self-diffusion constant vs. n_p/n_e. The solid triangles are the data of Antonietti, Folsch and Sillescu.[13] The solid curve is the fit of Eq. (3.13) to experiment. The matrix molecular weight was 111,000.

agreement with experiment throughout this transition region. The activation energy obtained from the value of d_0 at the two temperatures is about 30 kcal/mole.

4. Viscoelastic Response

In order to obtain a theory of the viscoelastic properties of a polymer melt that is in agreement with the experimental scaling behavior, Eq. (1.1b), we had to develop a somewhat more detailed model than was required for diffusion[24]. Three additional physical assumptions were necessary. They are in the spirit of those presented in Sect. 3 but go farther. The picture the reader should keep in mind is that the polymer melt is a dense network of entangled chains. When the polymer melt is subjected to a step deformation, there is resistance because the deformation drags the collection of chains into a new spatial configuration in a time fast compared to the internal relaxation processes. The deformed collection

of entangled chains is clearly out of equilibrium; it is the return of the network back to an equilibrium configuration which constitutes the viscoelastic response of the melt.

The physical assumptions we employ to describe this return to equilibrium are:

1) Taking our cue from experiment, we assume that the short time response of the melt is rubber like. Indeed this is the same assumption introduced into the reptation model by Doi and Edwards[3]. In particular, we assume (as they did) that the stress tensor $\sigma_{\alpha\beta}$ can be factored such that[5]

$$\sigma_{\alpha\beta}(t) = \sigma_{\alpha\beta}(t_e)\, F(t)\,, \tag{4.1}$$

where $\sigma_{\alpha\beta}(t_e)$ is a strain dependent quantity that depicts the short time network response of the melt and $F(t)$ is related to the long time configurational relaxation of the melt. Equation (4.1) assumes that on the average the stored energy is distributed uniformly along the chains and is consistent with the experimentally observed separability of the strain and time dependence seen in stress-strain relaxation experiments.[5]

We envisage this process to take place in the following steps: After the deformation, each chain faces a new set of dynamic entanglements which restricts their motion and return to equilibrium. Moreover, the chain contour length itself is out of equilibrium. The first relaxation process involves chain contour length equilibration where each chain flows through the loops produced by the dynamic entanglements. Since this process requires little if any dragging of other chains it should proceed rapidly and is the process probed by the plateau modulus. This relaxation process is completely analogous to the motion through the slip links of the Doi-Edwards theory,[3] except that we have identified the physical origin of these slip links as the dynamic entanglements.

At longer times, the chain contour can further relax by the network of entanglements as a whole relaxing (it is this latter relaxation that Doi and Edwards[3] attribute to reptation). This relaxation process takes place by the same type of motion that contributes to self diffusion, i.e. a chain drags the dynamic entanglements along with it.

In order to treat in a relatively simple fashion the long time relaxation of the network of chains involving a complicated many body entangled motion we must employ a trick. Think of a single entangled chain — in order for it to relax to equilibrium, the whole network of chains must also relax to an equilibrium configuration. Hence, we can use the relaxation of a typical average chain as a monitor of the relaxation of the network as a whole. That is, the relaxation of a single chain reports on the relaxation of the entire network of chains.

2) To model the long time relaxation of a single chain in the network of chains, we treat it as a Rouse chain which has, due to the effect of the dynamic entanglements, some slow moving points distributed along the chain. This is completely in the spirit of our treatment of diffusion. Since if one writes the diffu-

sion constant in terms of ζ_{av}, the mean friction constant per monomer is

$$D = k_B T / n\zeta_{av} . \tag{4.2a}$$

Equations (2.1) and (3.6) give

$$\zeta_{av} = \zeta_0 (1 + n/n_e) \tag{4.2b}$$

where ζ_0 is the Rouse friction constant per monomer in the absence of dynamic entanglements. Of course, in reality dynamic entanglements are constantly being destroyed by chains drifting apart, and new ones are constantly being created. The detailed kinetics is not presently known. Here, we neglect the explicit entanglement dynamics by replacing it with a static time average. To repeat — polymer chains in the melt are not Rouse chains with a few slow moving (i.e. high friction) points. They are a dynamically entangled network. However, the apparent motion of an average chain in the dynamically entangled melt is the same as the motion of a Rouse chain with slow moving points, and we can use the relaxation of this "average" model chain to report back the relaxation of the whole network.

To proceed further we must know how these slow moving points (i.e. dynamic entanglements) are distributed along the chain contour. Given the present state of computation, this is a very difficult quantity to obtain from simulation although we are presently attempting to extract meaningful results from the $n = 216$ homopolymeric case. Thus,

3) When n/n_e is on the order of one, the slow moving points are localized near the middle of the chain. As n/n_e increases, the fraction of the chain included between slow moving points approaches unity. Physically, this reflects the fact that the ends of a chain are more mobile than the center. Hence, contacts or entanglements which are near an end can easily disengage by the end moving away from the contacting chain. Since it is only long time contacts which contribute to the hydrodynamic properties, and these are considerably less probable near one end, we feel safe in disregarding this possibility. As the chain gets longer, the fraction of the chain consisting of the more mobile ends grows smaller and in the limit of infinitely long chains goes to zero. Hence, the fraction of the chain which is not an end and which can be the site of a slow moving point grows.

Fortunately, the qualitative behavior of the chains appears to be insensitive to the details of the distribution of dynamic entanglements. Several reasonable assumptions about the distribution give, at least qualitatively, the same results. Again, as in the treatment of diffusion, we shall present here only the most important results of the model. The interested reader should consult our original paper for the material omitted here.[24]

Before looking at the quantitative results of our model, we shall pause to examine some qualitative features that emerge. If we consider a melt of chains having a length on the order of the entanglement length, then each chain on the average has a single dynamic entanglement. Our model depicts the motions of an average chain as those of a Rouse chain with a single slow moving bead located near the center of the chain that has a large friction constant $\zeta = (n + 1)\,\zeta_o$. Thus, for this model chain, with its nonuniform distribution of friction constants, the center of mass, which depends on the mass distribution (which is uniform along the chain) is not coincident with the center of resistance which depends on the distribution of friction constants. An immediate consequence is that the center of mass motion and center of resistance motion differ, and there is a coupling between the internal motions of the chain and the external, center-of-mass, motion.

If we now consider the terminal relaxation time of the end to end vector, τ_R, for such a chain, we see that the slow moving bead in the center of the chain acts as a point defect and really has only a small effect on the motions of the ends. Hence, τ_R should be quite close to the terminal relaxation time of a pure (i.e. unentangled) Rouse chain of the same length in the same medium. On the other hand, if we look at the diffusional properties of our model chain, since it has twice the total friction of a pure Rouse chain (after all it is "pulling" another chain through the medium), it has a diffusion constant half as large as a pure Rouse chain. This qualitative argument suggests that the diffusion constant should approach its asymptotic, large molecular weight, entangled behavior at shorter chain lengths than does the terminal relaxation time. Thus, the product $D\tau_R/\langle S^2\rangle$ should scale as n^α where α is a monotonically decreasing function of n in accord with the simulation. This expectation is confirmed by the detailed calculations, see for example Fig. 13 of Ref. 24. Furthermore, if $\eta \propto \tau_R$ (as we shall show below), then D and η reach their asymptotic entangled behavior (where ultimately $\eta \sim n^3$) at quite different values of the chain length. This qualitative argument does not indicate whether n_c is greater or less than n_c'. However, as we shall show, our model indicates that the $\eta \sim n^{3.4}$ scaling results from the lag in τ_R reaching its asymptotic long chain entangled behavior and that $n_c' > n_c$.

From assumption (1) and following the procedure of Doi-Edwards[3] and Graessely[5,35] we rewrite Eq. (4.1) for the stress tensor of a polymer melt subject to a uniform shear deformation, $\gamma \ll 1$ (thus limiting our model to the linear viscoelastic regime) in the x direction as

$$\sigma_{xy}(t)/\gamma = G_N^0 F(t)$$

$$= G(t) \tag{4.3}$$

In Eq. (4.3), G_N^0 is the plateau modulus which is chain length independent and

$G(t)$ is the relaxation modulus. From the general theory of viscoelasticity[6] one can calculate the zero frequency shear viscosity from $G(t)$ by

$$\eta = \int_0^\infty dt\, G(t) dt \tag{4.4}$$

and the recoverable compliance as

$$J_e = \int_0^\infty dt\, t\, G(t)/\eta^2 . \tag{4.5}$$

From assumptions (2) and (3), we evaluate $F(t)$ in Eq. (4.3), by associating $F(t)$ with the configurational relaxation of an average (reporter) chain having some slow moving points. $F(t)$ is taken to be the normalized autocorrelation function of the radius of resistance vector $\mathbf{S}_r$. $\mathbf{S}_r$ is analogous to $\mathbf{S}$, the radius-of-gyration vector, but where the origin rather than being located at the center of mass is located at the center of resistance. Within the confines of assumption (3), we use several different distributions of dynamic entanglements to show that the results are qualitatively identical. A given distribution of slow moving points is generated by assuming that every bead has a monomeric friction constant ζ_0, but some of the beads have an additional friction constant proportional to n to mimic the effect of the dynamic entanglements.

Smeared friction constant model

The simplest case of the model is when the distribution of friction constants, $\{\zeta_i\}$, is replaced by the mean friction constant per bead ζ_{av} given in Eq. (4.2b). Physically, one would expect this to be a limiting case for any distribution in the limit of infinite chain length. That is, when the chain length gets very large compared to the average distance between dynamic entanglements, i.e. $n/n_e \to \infty$, one is justified in replacing the discrete distribution function by a continuum. Moreover, the viscosity for this model, which can be obtained as an analytic expression (as can the shear compliance), can be shown to be an upper bound to the viscosity obtained for a nonuniform distribution of friction constants.

Intuitively, one would expect that the energy dissipation of a chain would be greater when the total friction is spread out over the entire chain rather than if it is localized at a few sites; when the friction is localized, a normal mode can easily skip over these very slow moving points. However, when all points are fricitionally equivalent, one can no longer reduce the total friction (and hence lower the energy dissipation) by moving one bead rather than another. A more detailed discussion of the nature of this upper bound is given in Ref. 24. Physically, this means that in the long chain limit, the viscosity η approaches the viscosity of the smeared friction constant model η^0 from below.

Since the smeared friction constant model has a relaxation spectrum identical to that of a Rouse chain with a bead friction constant given by Eq. (4.2b), we use this relaxation spectrum in Eq. (4.3) yielding

$$\eta^0 = (\pi^2/15)\, G_N^0\, \tau_R^0\,, \tag{4.6}$$

where τ_R^0 is the relaxation time of the slowest relaxing Rouse mode (the end-to-end vector relaxation time). Thus, since G_N^0 is independent of chain length, when expressed in weight of chains/unit volume, the chain length dependence of the viscosity is given by the chain length dependence of τ_R^0. In the large n limit,

$$\lim_{n/n_e \to \infty} \tau_R^0 \sim \frac{n^3}{n_e}\,. \tag{4.7a}$$

Thus,

$$\eta^0 \sim n^3/n_e\,, \qquad n/n_e \to \infty\,, \tag{4.7b}$$

and the crossover exponent δ in $\eta^0 \sim n^\delta$ approaches 3 from below.

The smeared friction model does not yield the experimentally observed 3.4 power law scaling for viscosity[6,14], in this it agrees with the reptation model which also yields a cubic power law scaling. In fact, it can be easily shown that

$$\eta^0 = \frac{4}{15}\,\eta_{\text{reptation}}\,, \tag{4.8}$$

and thus it is somewhat closer to experimental results than the reptation model which predicts viscosities somewhat larger than are experimentally observed[5,35]. More sophisticated variants of the reptation model including tube length fluctuations by Doi[36] and subsequently by Rubinstein[37] have been found to numerically give rise to an apparent power law dependence of η in the neighborhood of 3.4. In the Doi model, η is predicted to asymptotically approach 3, whereas the Rubinstein model is not inconsistent with a power law dependence of η anywhere between about 3.2 and 3.5. The Doi functional form in particular gives a reasonable fit to experiment.[38]

Before going on to the more detailed distributions of dynamic entanglements, we point out that due to the bounding of η by η^0 from above discussed earlier, all models in this class have the asymptotic property that at high enough molecular weight they will yield a cubic scaling law for the viscosity. This is in qualitative agreement with the experiments of Colby, Fetters, and Graessley[38] on the molecular weight dependence of η in polybutadienes which can be (but need not

necessarily be) interpreted as showing that above an n/n_e of approximately 300, the experimentally observed 3.4 scaling behavior turns over into a cubic scaling law.

Distribution of slow moving points

To use a more realistic distribution of dynamic entanglements, we must resort to numerical computations. In particular, we must develop a normal mode description of the chain where the beads now have nonidentical friction constants. This involves diagonalizing matrices on the order of the chain length. In order to be able to obtain a large number of entanglements and still keep the size of the matrices manageable, we have set n_e, the distance between dynamic entanglements, at an artificially small value. Hence, when we use $n_e = 15$ (for example) one should think of each bead on the chain as representing approximately 10–20 physical monomer units.

We shall describe three different distributions of entanglements presented in order of an increasing sophistication of the distributions of $\{\zeta\}$ assumed. In all cases the total friction constant per molecule is $n\zeta_{av} = (1 + n/n_e)n\zeta_o$. Since this theory is really a theory of entangled chains, the short time behavior of $G(t)$ in the crossover regime from the free Rouse chain (where the assumption of a rubber-like short time response is incorrect) to the entangled chain behavior is beyond the scope of the present treatment. Hence we restrict ourselves to chain lengths $n \geq 3n_e$.

i) n-Independent spacing, identical slow moving point model.

In this simplest model, all n/n_e of the slow moving beads are uniformly distributed about the center of the chain, each having a friction constant

$$\zeta_i = (1 + n)\zeta_0 .$$

The remaining $n - n/n_e$ beads have a friction constant ζ_0. Because the beads are symmetrically distributed about the center, as n increases, the longest wavelength modes very quickly have most of their amplitudes concentrated on the high friction beads. Since the value of the viscosity is dominated by these longest wavelength modes, it quickly saturates to the smeared friction constant value. For example, if we fix $n_e = 15$ and vary the chain length we obtain: $n = 45$, $\eta/\eta^0 = 0.962$; $n = 90$, $\eta/\eta^0 = 0.989$; $n = 135$, $\eta/\eta^0 = 0.996$; $n = 180$, $\eta/\eta^0 = 0.997$. Since for a smeared friction constant distribution, $\eta \sim n^2 (1 + n/n_e)$, this implies that this equally spaced distribution has a power law behavior in the crossover region for the viscosity between 2 and 3 — which is incorrect. Physically, this arises because this distribution of slow moving points makes it very difficult to localize the effect of the slow moving points on the terminal relaxation time of the end-to-end vector, and it is just this localization at small n/n_e that we believe is

responsible for the greater than cubic power law scaling of the viscosity. So we shall now look at distributions which embody more of the physics.

ii) Extra slow center, n-independent spacing model

Here we assume that the central bead has the largest friction constant in the chain. This approximates the condition that the center of the chain moves the slowest. Therefore, since dynamic entanglements in this region should be the longest lived, the decreased mobility of this region should be greatest. Thus we give the central bead a friction constant of

$$\zeta = (1 + 3n)\zeta_0 .$$

The remaining $n/n_e - 3$ slow moving beads are almost equally spaced about the center and have equal friction constants,

$$\zeta = (1 + n)\zeta_0$$

and the $n - [(n/n_e) - 2]$ fast moving beads have a friction constant of ζ_0.

As we shall show below, the results of this distribution are qualitatively similar to the results obtained with our third distribution; thus, we shall present them together.

iii) Identical slow moving points, n-dependent spacing model

In this model, we look more closely at the nature of the dynamic entanglements. We assume that the friction constants of all the slow moving points are the same, but while keeping a uniform spacing we assume that the spacing distance, n_d, is chain length dependent. The reasoning behind this distribution is that for any chain, even a free isolated Rouse chain, the terminal relaxation increases with increasing chain length at least as fast as n^2 (the value for the Rouse chain). Thus, if a dynamic entanglement occurs at a position Δ beads away from the end in a chain of length n and in a chain of length $2n$, the entanglement in the chain of size $2n$ will have considerably more time to disengage. Hence, in our effective single particle picture, the entanglement closest to the end of the chain of length $2n$ should be farther from the end than for the chain of length n.

A model distribution encompassing this reasoning is obtained by uniformly distributing the n/n_e slow moving points about the center, each with a friction constant

$$\zeta = (1 + n)\zeta_o ,$$

such that the spacing between slow moving points is

$$n_d = n_e(1 - 2\,n_e/n) .$$

This places the slow moving bead closest to the end a distance $1.5\ n_e - n_e^2/n$ from the end bead. As n increases this distance increases and approaches an asymptotic value of $1.5\ n_e$, and the average spacing between dynamic entanglements n_d also increases approaching n_e asymptotically. Hence the model converges at large n to the n-independent spacing, identically slow moving point model. This model has the attractive and physically reasonable feature that for smaller chains the dynamic entanglements will on the average cluster closer to the center than for large chains.

Results

We will only present here the results for the calculation of the terminal relaxation time and the shear viscosity for the various models. Calculations of other quantities such as the center of mass autocorrelation function and the comparison of these quantities with the simulation results are given in detail in Ref. 24.

Figure 7 is a log-log plot of the relaxation time of the longest wavelength normal mode of the chain τ_R/t_0 vs n/n_e for the extra slow center distribution (open squares) and the identical slow moving point distribution (open triangles) (t_0 is

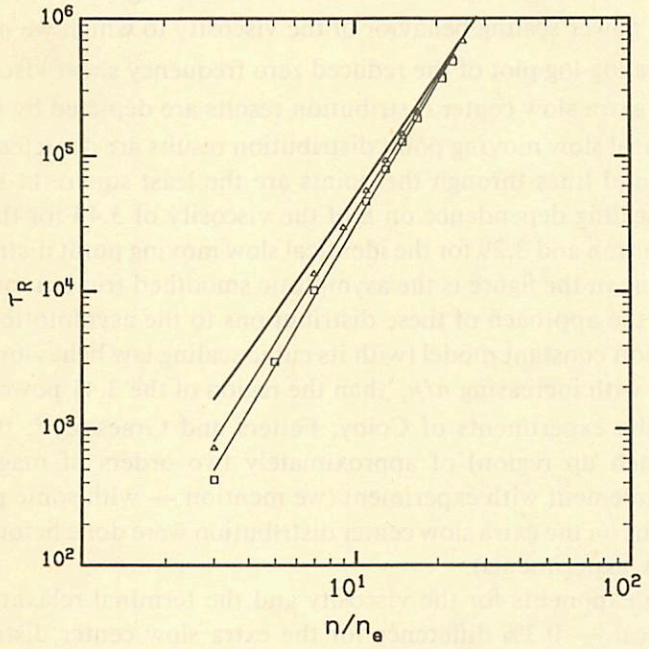

Fig. 7. Log-log plot of τ_R/t_0 vs. n/n_e for extra slow center distribution (open squares) and the identical slow moving point, n-dependent spacing distribution (open triangles). See text for further details. The solid lines are the least square fit to the points in each case. The curve without any symbols is the smeared friction constant model prediction.

the characteristic time it takes a monomer, in the medium of interest, to diffuse a root mean square distance equal to the root mean square distance between neighboring beads). The solid lines are a least square fit to the points. The solid line without any symbols is the smeared friction constant model prediction. The scaling exponent as a function of n for the terminal relaxation time is 3.43 for the extra slow center distribution and 3.21 for the identical slow moving point distribution. This deviation from a cubic scaling behavior reflects the ability of the longest wavelength mode to minimize the contribution of the slow moving points. That is, if there are not too many of them, it treats them as localized defects and effectively hops over them. If the large friction constant component is spread over all the beads, as in the smeared friction constant model, the effective friction constant per bead felt by the longest wavelength mode is larger. Hence, the terminal relaxation time is less than the terminal relaxation time for the smeared friction constant model. For example in the identical slow moving point distribution, when $n = 45$, $\tau_R/t_0 = 718.8$, while the smeared friction model gives a $\tau_R/t_0 = 1641.4$. Remember that asymptotically, for large n, the results from all the various distribution functions must approach those from the smeared friction constant model. Since at small n/n_e they start out with τ_R smaller than τ_R^0 (their asymptotic limit which they must approach at large n/n_e) τ_R must increase faster than τ_R^0 with increasing n/n_e. We view this transition region behavior as the origin of the 3.4 power scaling behavior of the viscosity to which we now turn.

Figure 8 is a log-log plot of the reduced zero frequency shear viscosity $\eta/G_N^0 t_0$ vs n/n_e. The extra slow center distribution results are depicted by open squares and the identical slow moving point distribution results are depicted by open triangles. The solid lines through the points are the least square fit straight lines leading to a scaling dependence on n of the viscosity of 3.44 for the extra-slow center distribution and 3.29 for the identical slow moving point distribution. The heavy solid line in the figure is the asymptotic smoothed friction model limiting result. While the approach of these distributions to the asymptotic value of the smeared friction constant model (with its cubic scaling law behavior) is probably slightly faster with increasing n/n_e than the region of the 3.41 power law scaling behavior in the experiments of Colby, Fetters and Graessley[38], the crossover region (or catch up region) of approximately two orders of magnitude is in qualitative agreement with experiment (we mention — with some pride — that the calculations on the extra slow center distribution were done before we became aware of these experiments).

The scaling exponents for the viscosity and the terminal relaxation time are almost identical — 0.3% difference for the extra slow center distribution and 2.4% difference for the identical slow moving point model. This suggests that we should be able to use the calculated terminal relaxation time to approximate the viscosity. This should be useful in simulations where it is relatively easy to calculate terminal relaxation times but quite difficult to calculate viscosities

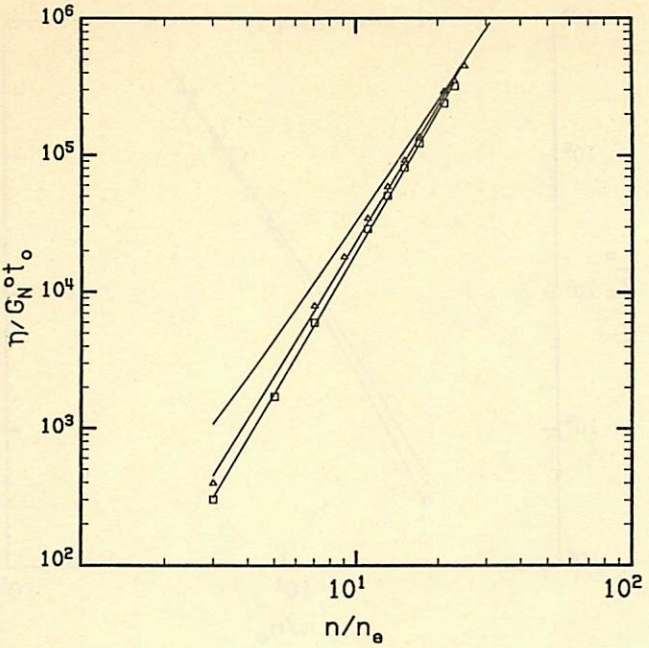

Fig. 8. Log-log plot of the reduced zero frequency shear viscosity, $\eta/G_N^0 t_0$, vs. n/n_e. The open squares (open triangles) are the extra slow center distribution (identical slow moving point, n dependent spacing distribution). The solid curve without any symbols is the smeared friction constant model prediction.

directly. To this end we try the approximate form suggested by Eq. (4.6) i.e. the correct result for a Rouse like smeared friction model

$$\eta_{\text{app}} = \left(\frac{\pi^2}{15}\right) G_N^0 \tau_R \,. \tag{4.9}$$

Results using this approximation are plotted in Fig. 9 where the open squares (open triangles) are the exact results using the extra slow center (identical slow moving point) model and the smooth curves are the result of using the approximate formula, Eq. (4.9). The agreement with the exact values is quite good, differing by about 20% when $n/n_e = 3$ and by about 1 percent when n/n_e is larger than 23.

Finally, we return to the question of the relative magnitude of the crossover degrees of polymerization for the diffusion constant (n_c') and the viscosity (n_c). Figures 8 and 9 show that the $\eta \sim n^{3.4}$ apparent power law behavior is well developed for n_c in the order of 3 n_e. Numerically, using Eq. (2.1), we find $D \sim d_0 n_e/n^2$ when n_c' equals about 7 n_e. Thus, the model reproduces the observed fact that $n_c' > n_c$.

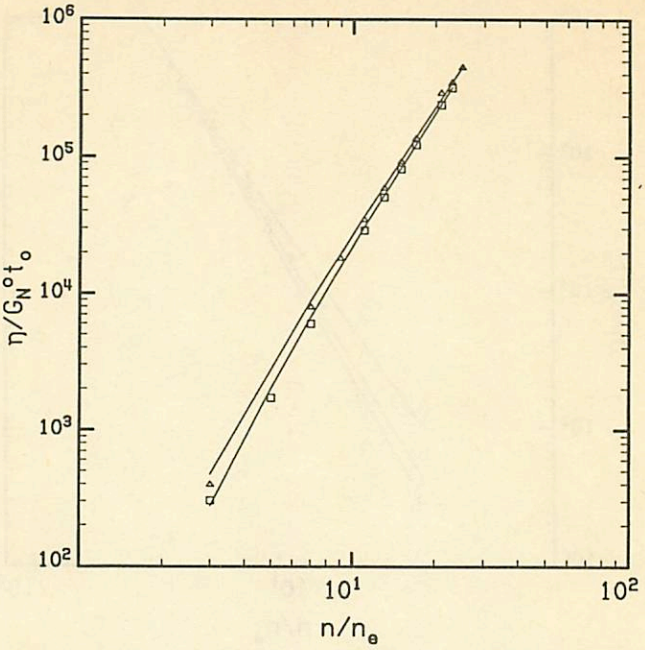

Fig. 9. Log-log plot of the reduced frequency shear viscosity, the open squares (open triangles) are the extra slow center (identical slow moving point, n dependent spacing distribution) results. The solid lines are generated using the approximate form of Eq. (4.9) with τ_R appropriate to each distribution.

5. Summary

We have shown that by using the insights obtained from computer simulations about the nature of dynamic entanglements in polymer melts, we have obtained a new theoretical model of polymer melts that is able to explain the experimental results.

The major features that we abstracted from the computational experiments and incorporated into our model are: i) polymer chains in a dense system do not reptate but rather appear to undergo isotropic motion; ii) most of the interchain contacts are very short lived, but iii) there are a small number of widely spaced (down a given chain) interchain contacts that persist for a long time — these contacts we refer to as dynamic entanglements. In our model it is these dynamic entanglements which produce the unusual scaling properties of long chain polymer melts.

The qualitative picture of chain motion that emerges is that in a polymer melt, the chains behave essentially like Rouse chains (i.e. the same behavior as in dilute solution) except that where there is a dynamic entanglement of two chains (recall such entanglements are dilute) the chains drag each other through solution. Thus the motion of an individual chain in solution looks like a Rouse chain with a

widely spaced distribution of slow moving — i.e. high friction constant points. It is these slow moving points which represent the effect of dragging another chain through the melt. Of course in reality these dynamic entanglements are continuously dissolving as chains diffuse apart, and new ones are forming as chains diffuse together. Thus, the picture we are presenting is really a statistically time averaged picture of this motion of an "average chain".

This picture of chain motion suffices to understand the diffusional motion of polymer chains in a melt. It produces the correct scaling behavior of the diffusion constant ($D \sim n^{-1}$ for small chain lengths going over to n^{-2} for longer chains). It also suggests that the glass transition for high molecular weight polymers occurs when dynamic entanglements become kinetically trapped and can no longer disengage. Short unentangled polymers, which do not have the entanglement trapping mechanism available, undergo a glass transition when the local conformational changing volume fluctuations freeze out.

In order to understand the viscoelastic behavior of polymer melts, we must realize that when we subject the melt to a shear deformation we are probing the return of the perturbed entangled network of polymer chains to an equilibrium configuration. For short times after the deformation, the entanglements act like crosslinks in a rubber. For longer times, we can use our picture of the motion of an average entangled chain as a probe of the relaxation process of the entangled network. That is, the average chain can only relax as the network as a whole relaxes, and hence the average chain's relaxation reports back to us the relaxation of the whole entangled polymer melt. This model predicts that the viscosity scales as n for low molecular weight polymers and eventually goes over to an asymptotic n^3 behavior for high molecular weight polymers. In the crossover region, which covers several decades of molecular weight, the relaxation is trying to catch up with its asymptotic behavior. In this long crossover (or catch up) regime the model produces the hitherto puzzling $n^{3.4}$ power scaling behavior of the viscosity. This three-regime picture of polymer melt viscosities is in agreement with Colby, Fetters and Graessley's recent experimental results[38]. Hence, our model strongly suggests that the 3.4 power scaling law for viscosity should be viewed as ubiquitous but not fundamental.

The model also easily produces the different crossover molecular weights from entangled to unentangled behavior for diffusion and viscosity.

Lastly we should mention that, although we have not shown it here, the model also explains in a physical manner the various time regimes of the mean square bead displacements seen in the simulations.

Hence the simple physical picture we have presented seems to encompass the necessary physics to understand the dynamics involved in the transport properties of polymer melts. So while this model is by no means a complete theory of polymer melts — such a complete theory would have to yield for example the distribution of entanglements — it should prove useful in improving our understanding of the dynamic processes in polymer melts and dense polymer solutions.

Acknowledgments

This research was supported in part by a grant from the polymer program of the National Science Foundation No. DMR 85-20789. The contribution of Dr. A. T. Yeates in preparing Figs. 5 and 6 is gratefully appreciated.

References

1. P. G. de Gennes, *J. Chem. Phys.* **55** (1971) 572.
2. P. G. de Gennes, *Scaling Concepts in Polymer Physics* (Cornell University, NY, 1979).
3. M. Doi and S. F. Edwards, *J. Chem. Soc. Faraday Trans. 2*, **74** (a) 1789; (b) 1802; (c) 1818 (1978); (d) **75** (1978) 38; (e) *The Theory of Polymer Dynamics* (Clarendon Press, Oxford, 1986).
4. W. W. Graessley, *Adv. Polym. Sci.* **16** (1974) 1.
5. W. W. Graessley, *Adv. Polym. Sci.* **47** (1982) 67.
6. J. D. Ferry, *Viscoelastic Properties of Polymers* (Wiley, NY, 1980).
7. P. F. Green, P. J. Mills, C. J. Palmstrom, J. W. Mayer and E. J. Kramer, *Phys. Rev. Lett.* **53** (1984) 2145.
8. P. F. Green and E. J. Kramer, *Macromolecules* **19** (1986) 1108.
9. M. Antonietti, J. Coutandin, R. Grütter, and H. Sillescu, *Macromolecules* **17** (1984) 798.
10. M. Antonietti, J. Coutandin and H. Sillescu, *Macromolecules* **19** (1986) 793.
11. M. Tirrell, *Rubber Chem. Tech.* **57** (1984) 523.
12. C. R. Bartels, B. Crist and W. W. Graessley, *Macromolecules* **17** (1984) 2702.
13. M. Antonietti, K. J. Folsch, and H. Sillescu, *Makromol. Chem.* **188** (1987) 2317.
14. G. C. Berry and T. G. Fox, *Adv. Polymer Sci.* **5** (1968) 261.
15. P. E. Rouse, *J. Chem. Phys.* **21** (1955) 1272.
16. H. Yamakawa, *Modern Theory of Polymer Solutions* (Harper & Row, NY, 1969 chap. 6.
17. K. F. Freed, in *Progress in Liquid Physics*, ed. C. A. Croxton (Wiley, NY, 1978), p. 343.
18. J. Klein, *Macromolecules* (a) **11** (1978) 852; (b) **19** (1984) 105.
19. M. Daoud and P. G. de Gennes, *J. Polym. Sci. Polym. Phys. Ed.* **17** (1979) 1971.
20. M. Doi, *J. Poly. Sci., Polym. Lett. Ed.* **19** (1981) 265.
21. A. Kolinski, J. Skolnick and R. Yaris, *J. Chem. Phys.* (a) **84** (1986) 1922; (b) **86** (1987) 1567; (c) **86** (1987) 7164; (d) **86** (1987) 7174.
22. J. Skolnick, A. Kolinski, and R. Yaris, *Accts. Chem. Res.* **20** (1987) 350.
23. J. Skolnick, R. Yaris and A. Kolinski, *J. Chem. Phys.* **88** (1988) 1407.
24. J. Skolnick and R. Yaris, *J. Chem. Phys.* **88** (1988) 1418.
25. S. F. Edwards, *Polymer* **6** (1977) 143.
26. K. E. Evans and S. F. Edwards, *J. Chem. Soc. Faraday Trans. 2* **77** (1981) 1891, 1929.
27. S. F. Edwards and K. E. Evans, *J. Chem. Soc. Faraday Trans. 2* **77** (1981) 1913.
28. A. Baumgartner and K. Binder, *J. Chem. Phys.* **75** (1981) 2994.
29. M. Bishop, D. Ceperley, H. L. Frisch, and M. H. Kalos, *J. Chem. Phys.* **76** (1982) 1557.
30. K. Kremer, G. S. Grest, and I. Carmesin, *Phys. Rev. Lett.* **61** (1988) 566.
31. W. Hess, *Macromolecules* **19** (1986) 1395.
32. J. Lamb, in *Molecular Basis of Transitions and Relaxations*, Midland Macromolecular Monographs, ed. D. J. Meier (Gordon and Breach, NY, 1978), Vol. 4, p. 52.
33. T. G. Fox and P. J. Flory, *J. Appl. Phys.* **21** (1950) 581.
34. A. T. Yeates, J. Skolnick and R. Yaris, *J. Polym. Sci. Poly. Phys. Ed.*, (to be published).
35. W. W. Graessley, *J. Polym. Sci. Poly. Phys. Ed.* **18** (1980) 27.
36. M. Doi, *J. Polym. Sci. Poly. Phys. Ed.* **19** (1981) 265.
37. M. Rubinstein, *Phys. Rev. Lett.* **59** (1987) 1946.
38. R. H. Colby, L. J. Fetters and W. W. Graessley, *Macromolecules* **20** (1987) 2226.